Dear Author

Here are the proofs of your article.

- You can submit your corrections **online** or by **fax**.
- For **online** submission please insert your corrections in the online correction form. Always indicate the line number to which the correction refers.
- Please return your proof together with the permission to publish confirmation.
- For **fax** submission, please ensure that your corrections are clearly legible. Use a fine black pen and write the correction in the margin, not too close to the edge of the page.
- Remember to note the journal title, article number, and your name when sending your response via e-mail, fax or regular mail.
- **Check** the metadata sheet to make sure that the header information, especially author names and the corresponding affiliations are correctly shown.
- **Check** the questions that may have arisen during copy editing and insert your answers/corrections.
- **Check** that the text is complete and that all figures, tables and their legends are included. Also check the accuracy of special characters, equations, and electronic supplementary material if applicable. If necessary refer to the *Edited manuscript*.
- The publication of inaccurate data such as dosages and units can have serious consequences. Please take particular care that all such details are correct.
- Please **do not** make changes that involve only matters of style. We have generally introduced forms that follow the journal's style.
  Substantial changes in content, e.g., new results, corrected values, title and authorship are not allowed without the approval of the responsible editor. In such a case, please contact the Editorial Office and return his/her consent together with the proof.
- If we do not receive your corrections **within 48 hours**, we will send you a reminder.

Please note

Your article will be published **Online First** approximately one week after receipt of your corrected proofs. This is the **official first publication** citable with the DOI. **Further changes are, therefore, not possible.**

After online publication, subscribers (personal/institutional) to this journal will have access to the complete article via the DOI using the URL:

`http://dx.doi.org/10.1007/s11356-020-08857-3`

If you would like to know when your article has been published online, take advantage of our free alert service. For registration and further information, go to: http://www.springerlink.com.

Due to the electronic nature of the procedure, the manuscript and the original figures will only be returned to you on special request. When you return your corrections, please inform us, if you would like to have these documents returned.

The **printed version** will follow in a forthcoming issue.

Metadata of the article that will be visualized in OnlineFirst

1	Article Title	**Assessing chromium pollution and natural stabilization processes in agricultural soils by bulk and micro X-ray analyses**	
2	Article Sub- Title		
3	Article Copyright - Year	**Springer-Verlag GmbH Germany, part of Springer Nature 2020 (This will be the copyright line in the final PDF)**	
4	Journal Name	Environmental Science and Pollution Research	
5	Corresponding Author	Family Name	**Gattullo**
6		Particle	
7		Given Name	**Concetta Eliana**
8		Suffix	
9		Organization	University of Bari "A. Moro"
10		Division	Department of Soil, Plant and Food Sciences
11		Address	Via G. Amendola n. 165/A, Bari 70126, Italy
12		e-mail	concettaeliana.gattullo@uniba.it
13	Author	Family Name	**Allegretta**
14		Particle	
15		Given Name	**Ignazio**
16		Suffix	
17		Organization	University of Bari "A. Moro"
18		Division	Department of Soil, Plant and Food Sciences
19		Address	Via G. Amendola n. 165/A, Bari 70126, Italy
20		e-mail	
21	Author	Family Name	**Porfido**
22		Particle	
23		Given Name	**Carlo**
24		Suffix	
25		Organization	University of Bari "A. Moro"
26		Division	Department of Soil, Plant and Food Sciences
27		Address	Via G. Amendola n. 165/A, Bari 70126, Italy
28		e-mail	
29	Author	Family Name	**Rascio**
30		Particle	
31		Given Name	**Ida**

32		Suffix	
33		Organization	University of Bari "A. Moro"
34		Division	Department of Soil, Plant and Food Sciences
35		Address	Via G. Amendola n. 165/A, Bari 70126, Italy
36		e-mail	
37	Author	Family Name	**Spagnuolo**
38		Particle	
39		Given Name	**Matteo**
40		Suffix	
41		Organization	University of Bari "A. Moro"
42		Division	Department of Soil, Plant and Food Sciences
43		Address	Via G. Amendola n. 165/A, Bari 70126, Italy
44		e-mail	
45	Author	Family Name	**Terzano**
46		Particle	
47		Given Name	**Roberto**
48		Suffix	
49		Organization	University of Bari "A. Moro"
50		Division	Department of Soil, Plant and Food Sciences
51		Address	Via G. Amendola n. 165/A, Bari 70126, Italy
52		e-mail	

53	Schedule	Received	6 December 2019
54		Revised	
55		Accepted	13 April 2020

56 Abstract

A combined approach based on multiple X-ray analytical techniques and conventional methods was adopted to investigate the distribution and speciation of Cr in a polluted agricultural soil, from the bulk-scale down to the (sub)micro-level. Soil samples were collected from two different points, together with a control sample taken from a nearby unpolluted site. The bulk characterization revealed that the polluted soils contained much higher concentrations of organic matter (OM) and potentially toxic elements (PTEs) than the control. Chromium was the most abundant PTE (up to 5160 g kg^{-1}), and was present only as Cr(III), as its oxidation to Cr(VI) was hindered by the high OM content. According to sequential extractions, Cr was mainly associated to the soil oxidisable fraction (74%) and to the residual fraction (25%). The amount of Cr potentially bioavailable for plant uptake (DTPA-extractable) was negligible. Characterization of soil thin sections by micro X-ray fluorescence (μXRF) and field emission scanning electron microscopy coupled with microanalysis (FEGSEM-EDX) showed that Cr was mainly distributed in aggregates ranging from tens micrometres to few millimetres in size. These aggregates were coated with an aluminosilicate layer and contained, in the inner part, Cr, Ca, Zn, P, S and Fe. Hyperspectral elaboration of μXRF data revealed that polluted soils were characterised by an exogenous

		organic-rich fraction containing Cr (not present in the control), and an endogenous aluminosilicate fraction (present also in the control), coating the Cr-containing aggregates. Analyses by high-resolution micro X-ray computed tomography (μCT) revealed a different morphology of the soil aggregates in polluted soils compared with the control. The finding of microscopic leather residues, combined with the results of bulk- and micro-characterizations, suggested that Cr pollution was likely ascribable to soil amendment with tannery waste-derived matrices. However, over the years, a natural process of Cr stabilization occurred in the soil thus reducing the environmental risks.
57	Keywords separated by ' - '	Chromium speciation - Soil pollution - Potentially toxic elements - X-ray fluorescence spectroscopy - μXRF - FEGSEM-EDX - μCT - Sequential extractions
58	Foot note information	Responsible Editor: Philippe Garrigues Springer Nature remains neutral with regard to jurisdictional claims in published maps and institutional affiliations.

Environmental Science and Pollution Research
https://doi.org/10.1007/s11356-020-08857-3

RESEARCH ARTICLE

Assessing chromium pollution and natural stabilization processes in agricultural soils by bulk and micro X-ray analyses

Concetta Eliana Gattullo[1] · Ignazio Allegretta[1] · Carlo Porfido[1] · Ida Rascio[1] · Matteo Spagnuolo[1] · Roberto Terzano[1]

Received: 6 December 2019 / Accepted: 13 April 2020

Abstract

A combined approach based on multiple X-ray analytical techniques and conventional methods was adopted to investigate the distribution and speciation of Cr in a polluted agricultural soil, from the bulk-scale down to the (sub)micro-level. Soil samples were collected from two different points, together with a control sample taken from a nearby unpolluted site. The bulk characterization revealed that the polluted soils contained much higher concentrations of organic matter (OM) and potentially toxic elements (PTEs) than the control. Chromium was the most abundant PTE (up to 5160 g kg^{-1}), and was present only as Cr(III), as its oxidation to Cr(VI) was hindered by the high OM content. According to sequential extractions, Cr was mainly associated to the soil oxidisable fraction (74%) and to the residual fraction (25%). The amount of Cr potentially bioavailable for plant uptake (DTPA-extractable) was negligible. Characterization of soil thin sections by micro X-ray fluorescence (μXRF) and field emission scanning electron microscopy coupled with microanalysis (FEGSEM-EDX) showed that Cr was mainly distributed in aggregates ranging from tens micrometres to few millimetres in size. These aggregates were coated with an aluminosilicate layer and contained, in the inner part, Cr, Ca, Zn, P, S and Fe. Hyperspectral elaboration of μXRF data revealed that polluted soils were characterised by an exogenous organic-rich fraction containing Cr (not present in the control), and an endogenous aluminosilicate fraction (present also in the control), coating the Cr-containing aggregates. Analyses by high-resolution micro X-ray computed tomography (μCT) revealed a different morphology of the soil aggregates in polluted soils compared with the control. The finding of microscopic leather residues, combined with the results of bulk- and micro-characterizations, suggested that Cr pollution was likely ascribable to soil amendment with tannery waste-derived matrices. However, over the years, a natural process of Cr stabilization occurred in the soil thus reducing the environmental risks.

Keywords Chromium speciation · Soil pollution · Potentially toxic elements · X-ray fluorescence spectroscopy · μXRF · FEGSEM-EDX · μCT · Sequential extractions

Introduction

Chromium (Cr) is a potentially toxic element (PTE) existing in soils both naturally and anthropogenically. Lithogenic Cr is considered being inert and non-hazardous, and may be found in weathered parent materials, as in chromite, or in clay minerals as substituent of octahedrally coordinated Al (Bartlett and James 1996; Becquer et al. 2003; Oze et al. 2004). Conversely, Cr of anthropogenic origin is of concern, especially when present in the hexavalent form [Cr(VI)]. Chromium toxicity in soil depends on the metal speciation between the hexavalent form and the trivalent one. These two Cr oxidation states differ for their physico-chemical properties and biological effects (Gattullo et al. 2018a). Trivalent Cr [Cr(III)] is almost immobile in soil at pH ranging between 4 and 8, due to its strong affinity for negatively charged ions and colloids (Dhal et al. 2013). In near neutral soils, Cr(III) is mainly precipitated as hydroxide [$Cr(OH)_3$] (Morrison et al. 2015). Trivalent Cr is essential for humans and animals, being involved in the sugar, protein and lipid metabolism, but it is not required by plants and microorganisms (Shahid et al. 2017). On the opposite, Cr(VI) exists in soil as soluble anionic forms (chromate and dichromate), and is extremely bioavailable and toxic to living organisms (Cook 2000; Ertani et al.

Responsible Editor: Philippe Garrigues

✉ Concetta Eliana Gattullo
concettaeliana.gattullo@uniba.it

[1] Department of Soil, Plant and Food Sciences, University of Bari "A. Moro", Via G. Amendola n. 165/A, 70126 Bari, Italy

JnlID 11356_ArtID 8857_Proof# 1 - 18/04/2020

2017). Partitioning of Cr between these two valence states depends on soil properties, especially pH, redox potential, organic matter content and amounts of manganese (Mn) and iron (Fe) oxides (Bartlett 1997; Dhal et al. 2013).

Soil pollution by Cr and, more generally, PTE has remarkably increased over the last decades even in the rural areas, because of intensification of crop systems, overuse of pesticides and fertilizers, and agronomical reuse of treated wastes and by-products of industrial and civil activities. In particular, Cr pollution of soils is mainly caused by disposal of chromite-ore processing residues and tannery wastes, while soil amendment with sewage sludge is considered the main cause of Cr enrichment in agricultural soils (Kabata-Pendias and Mukherjee 2007). Pollution of agricultural soils arouses great concern due to risks of transferring contaminants from soil to plants and, over the food chain, to livestock and humans. Uptake, translocation and accumulation of Cr by plants depend on the metal speciation (Shanker et al. 2005). Both Cr(VI) and Cr(III) can be absorbed by plant roots, then root reductases may reduce Cr(VI) to Cr(III); the latter is finally retained in root apoplast or stored in vacuoles of root cortex cells (Shanker et al. 2005; Barceló and Poschenrieder 1997). Despite Cr translocation from roots to shoots is very limited, Cr accumulation in the aerial part may become relevant if the amount of Cr(VI) absorbed exceeds the reducing capacity of root cortex cells (Barceló and Poschenrieder 1997).

Investigation of speciation, spatial distribution and stabilization processes of Cr in soil requires the use of analytical techniques able to solve the high complexity of the soil matrix with a spatial resolution down to the micrometre- or even nanometre-scale. In the last decades, X-ray-based analytical techniques have been advantageously applied to study the biogeochemistry of both essential and toxic elements directly in soil, with a minimum sample handling, and using a micrometre or nanometre resolution (Terzano et al. 2007; Thouin et al. 2016; Allegretta et al. 2018; Mehta et al. 2019; Terzano et al. 2019).

Among laboratory instruments available, micro X-ray fluorescence (μXRF), scanning electron microscopy coupled with chemical analysis (SEM-EDX) and micro X-ray computed tomography (μCT) offer extremely powerful tools for soil microanalysis. Micro-XRF is useful to map the elemental distribution and associations of elements in soil; SEM-EDX reveals the chemical composition and elemental distribution in soil together with the soil microstructure and morphology, while μCT provides 3-D images of soil particles with a submicrometre spatial resolution. In addition, other bulk X-ray analytical methods, such as energy-dispersive (ED-XRF) and wavelength dispersive (WD-XRF) X-ray fluorescence spectroscopies, allow rapid and non-destructive multielemental analyses of soils (Vanhoof et al. 2004), while X-ray powder diffraction (XRPD) enables investigating soil mineralogy.

X-ray analyses and microanalyses can be combined with more simple and traditional approaches assessing PTE fractionation in soil, such as single or sequential extraction procedures (SEP). SEP methods have been largely employed for studying the chemical forms and associations of PTE with the different soil components, notwithstanding the operational artefacts, limited selectivity of extracting agents and potential redistribution phenomena (Lombi and Susini 2009; Majumdar et al. 2012).

In the present study, a combined approach based on selective extraction methods and multiple X-ray analytical techniques was adopted to investigate the microscale and bulk-scale distribution of Cr in a PTE-polluted agricultural soil. Association of Cr with other elements was explored, as well as its interaction with soil solid components. The pool of information obtained was useful to link the microscale chemical speciation of Cr to its bulk behaviour, allowing to evaluate the potential availability and toxicity of this contaminant. Hypotheses about the origin of Cr pollution in the investigated soils are also presented.

Materials and methods

Soil sampling

The investigated site was located in the south of Italy (Altamura, Bari), in an agricultural area traditionally cultivated with durum wheat (*Triticum durum* Desf.). Monoculture of durum wheat was interrupted every 3 years by 1 year of set-aside or, alternatively, by 1 year of cultivation of a leguminous species. Soil was subjected to conventional tillage, regularly fertilized with N and P, and amended with organic matrices until 10–15 years ago. Information about type and doses of the organic amendment is not available. The investigated area, which extended approximately 1 ha, was preliminarily divided in ten subunits. A portable energy-dispersive X-ray fluorescence spectrometer (ED-XRF; NITON XL3t GOLDD, Thermo Scientific), equipped with an Ag target (50 kV, 40 μA), was used for measuring the concentrations of PTE in each subunit, acquiring three measurements on an area of about 4 m^2 previously selected in each subunit. Chromium was the most abundant PTE in soil, with concentrations up to 30 times higher than the national regulatory threshold for agricultural sites (150 mg kg^{-1}; Italian Directive n. 152/2006). The two subunits characterized by the lowest (soil A1) and highest (soil A2) Cr average concentration were selected. For both of them, a composite sample of disturbed soil was obtained by mixing three sub-samples collected in the 4-m^2 area, at 0–10-cm depth, using a plastic shovel. An additional soil sample was collected in an unpolluted farmland next to the polluted site, and used as control. Soil sampling was carried out at the beginning of July, about 3 weeks after wheat harvest.

Bulk soil characterization

Physical, chemical and mineralogical characterization

Soil samples were air-dried, sieved at 2 mm and characterized for texture, pH (KCl), electrical conductivity (EC), organic C content, total N content, total and active $CaCO_3$, available P, cation exchange capacity (CEC) and exchangeable bases, according to standard methodologies of soil analysis (Sparks 1996). Soil texture was determined with the modified pipette method (Indorante et al. 1990).

A representative aliquot (100 g) of each soil sample was pulverized with an agate mortar and pestle, and analysed for both the elemental and mineralogical composition by X-ray techniques. The major element content was measured by a wavelength dispersive X-ray fluorescence spectrometer (WD-XRF; Supermini 200, Rigaku Corporation, Tokyo, Japan), equipped with a Pd tube (50 kV, 4 mA, 200 W) and operating under vacuum. The instrument was preliminarily calibrated using a number of geological standards, as described by Allegretta et al. (2018). Analyses were performed on soil pellets obtained mixing 5 g of pulverized soil with 2 mL of Elvacite® 2046 (PanAnalytical) solution, which was dissolved in acetone at a concentration of 15% (w/w, resin/acetone).

The trace element content was measured by ED-XRF (NITON XL3t GOLDD with laboratory stand, Thermo Scientific). Analytical accuracy was evaluated analysing the standard reference materials BCR-CRM 038 (coal fly ash) and CCRMP TILL-4 (soil). Each sample was placed in an X-ray fluorescence sample cup (Fluxana, Germany) closed with a thin polypropylene membrane (Premier Lab Supply, USA), and analysed in triplicate. Due to the high ED-XRF detection limit for Cd, the quantification of this element was performed by inductively coupled plasma–atomic emission spectrometry (ICP-AES; Thermo iCAP 6000 series, Thermo Fisher Scientific Inc., Waltham, USA) after acidic digestion of the sample. Briefly, an aliquot of 100 mg of soil was pre-digested overnight in PTFE tubes using a mixture of 6 mL HNO_3 (70%), 1 mL HCl (37%) and 1 mL H_2O_2 (30%) (all reagents Trace Select, Sigma Aldrich), and then digested in a microwave oven (Multiwave GO, Anton Paar, Graz, Austria). Quantification by ICP-AES was performed in triplicate.

The concentration of Cr(VI) in soil was determined through the alkaline digestion of soil samples (USEPA, Method 3060A 1996), followed by the colorimetric assay with diphenylcarbazide (USEPA, Method 7196A 1992). Moreover, Cr(III)-net oxidation potential of soils was measured according to Bartlett and James (1996).

Soil mineralogical analysis was performed by X-ray powder diffraction (XRPD), using a Miniflex II X-ray diffractometer (Rigaku Corporation, Tokyo, Japan) equipped with a Cu-Kα X-ray source (30 kV, 15 mA, 450 W). Semiquantitative analyses were performed following the procedure described by Gattullo et al. (2018b). Briefly, pulverized soil was homogenized with 20% (w/w) of corundum (MicropolishTM II, 1 μm, Buehler, USA), used as the internal standard. Data were acquired between 3° and 120° 2 , with a step width of 0.02° and a counting time of 3 s per step. Analysis of XRPD data was carried out according to Gualtieri (2000), combining the Rietveld and reference intensity ratio (RIR) methods.

PTE fractionation and availability in soils

The plant available fraction of PTE was estimated by soil extraction with diethylenetriaminepentaacetic acid (DTPA) solution (0.005 M DTPA, 0.01 M $CaCl_2$, 0.1 M triethanolamine, pH = 7.3) (Lindsay and Norwell 1978).

Distribution of PTE in soil fractions characterized by increasing stability was evaluated using a modified BCR SEP (Sahuquillo et al. 1999), as described by Gattullo et al. (2018a). Briefly, four extraction steps were performed in sequence to assess the following: (1) PTE exchangeable fraction (1 M $MgCl_2$ at pH = 7); (2) PTE acid-soluble fraction (0.11 M acetic acid); (3) PTE reducible fraction (0.5 M hydroxylamine hydrochloride at pH = 2); (4) PTE oxidisable fraction (1 M ammonium acetate at pH = 2 after two oxidation steps with H_2O_2). Finally, the soil residue was air-dried and mineralised, as described above. The total concentrations of PTE in DTPA extracts and in fractions obtained at the end of each SEP phase were determined by ICP-AES (Thermo iCAP 6000 series, Thermo Fisher Scientific Inc., Waltham, USA).

Distribution of PTE in three different granulometric fractions was also investigated. The soil sieved at 2 mm (50 g) was sequentially dry-sieved at 500 μm and 125 μm, obtaining three granulometric classes: (1) 2000–500 μm; (2) 500–125 μm; (3) < 125 μm. The total concentration of PTE in each soil fraction was determined by ED-XRF, as previously described.

Soil characterization at the microscale

Soil thin sections (30-μm thickness), prepared after embedding the 2-mm-sieved soil in epoxy resin (L.R. White Resin, Polyscience Europe GmbH, Germany) (Allegretta et al. 2018), were analysed with a benchtop micro X-ray fluorescence spectrometer (μXRF; M4 Tornado, Bruker Nano GmbH, Germany). Elemental distribution maps were acquired under vacuum (20 mbar) using a Rh tube X-ray source (50 kV, 600 μA, 30 W) with policapillary optics and two 30 mm^2 XFlash® silicon drift detectors. X-ray maps were collected with a spot size of 25 μm, a step size of 25 μm and an acquisition time of 100 ms per pixel. X-ray fluorescence hyperspectral data were processed using both Bruker M4 software and a combination of the PyMca 5.1.3 (Solé et al. 2007) and Datamuncher (Alfeld and Janssens 2015) softwares.

JnlID 11356_ArtID 8857_Proof# 1 - 18/04/2020

Further analyses of soil thin sections were performed by field emission scanning gun electron microscopy coupled with microanalysis (FEGSEM-EDX, Zeiss Σigma SUPRA 300 VP, Carl Zeiss NTS GmbH, Germany), in order to elucidate the chemical and microstructural properties of soil aggregates containing high levels of PTE. The instrument was equipped with an EDX C-MaxN SDD spectrometer with an active area of 20 mm^2 (Oxford Instruments), and operated at 15 kV.

Soil aggregates of millimetric size were selected from each soil sample and analysed by high-resolution micro X-ray computed tomography (μCT, SkyScan 1272, Bruker Gmbh, Germany), operating at 60 kV and 166 mA. Analyses were performed using a 0.25-mm Al filter to improve the signal to noise ratio, and selecting a pixel size of 0.5 μm, a rotation step of 0.2° (0–180°) and an exposure time of 3000 ms.

Results and discussion

Bulk characterization of soils

Physical, chemical and mineralogical properties of soils

The three investigated soils were classified as Calcaric Leptosols, according to WRB classification (IUSS Working Group WRB 2006). Polluted soils (A1 and A2) were characterized by similar physico-chemical properties (Table 1). Compared with the control, they showed much higher values of organic C, total N, available P and CEC. All these parameters are indicative of a considerable enrichment of OM in A1 and A2 (21.4% and 23.4%, respectively), which is only partially attributable to the presence of degraded crop residues in the first centimetres of soil. Indeed, crop residues were present also in the control soil; however, the latter possessed 64% less OM than both polluted soils. The abnormal OM content of A1 and A2 possibly derived from soil amendment with recalcitrant organic fractions, most likely at doses exceeding the microbial degradation capacity of the soils. The higher EC of the two polluted soils, with respect to the control, may be attributed to soil amendment with organic matrices characterized by high EC values, such as sewage sludge (Wong et al. 2001). Soils showed similar texture, in particular A1 and A2 possessed a silt-loam texture (according to the USDA classification system), while the control was characterized by a silty clay loam texture. The three soils were strongly calcareous and characterized by a low (control), medium high (A1) and very high (A2) content of active carbonates; they showed a weakly alkaline pH.

The mineralogical composition was qualitatively similar for the three soils, and characterized by illite, kaolinite, quartz, calcite, albite, rutile and other amorphous components (Table 2). The latter comprise non-ordered and low-ordered phases, as well as minerals whose concentrations are below the XRPD detection limit. From the quantitative point of view, A1 and A2 differed from the control being richer in calcite (33% more, on average) and amorphous phases (35% more, on average), but poorer in clay minerals (45% less, on average) and quartz (38% less, on average). The higher amount of amorphous phases in A1 and A2 can be almost completely ascribed to the higher OM content (21.4% and 23.4%, respectively), as compared with the control (8.1%) (Table 1). Only slight mineralogical differences were detected between A1 and A2; in particular, A1 was characterized by a slightly higher content of illite and lower content of kaolinite and calcite. No pure PTE or Cr-bearing minerals were detected by XRPD in the soils under investigation.

The major-element composition of the two polluted soils slightly differed with respect to that of control, if data were normalized to the loss on ignition (LOI) content (Table 3). Values of LOI in A1 and A2 were approximately double than in the control, as predictable by the values of OM and total carbonate content of the three soils. As for major elements, A1 and A2 showed similar compositions, although the content of P_2O_5, SO_3 and CaO in A2 was slightly higher than in A1.

Concentrations of trace elements in the control, except for As, were below the maximum admissible limits reported by the Italian regulation for agricultural sites (Italian Directive n. 152/ 2006), thus confirming that this soil can be classified as unpolluted (Table 3). The level of As found in the control fell within the range reported in literature as background geochemical concentrations for Apulian agricultural soils (20–

t1.1 **Table 1** Physico-chemical properties of the polluted soils (A1 and A2) and control (unpolluted)

t1.2 t1.3 Soil	Texture	pH (H_2O)	pH (KCl)	EC μS cm^{-1}	OC^a g kg^{-1}	OM^b	Total N	Total $CaCO_3$	Active $CaCO_3$	$P_{Available}$ mg kg^{-1}	CEC $cmol_{(+)}$ kg^{-1}	Ca^{2+}	Mg^{2+}	Na^+	K^+
t1.4 Control	Silty clay loam	7.4	7.3	133	47	81	4	165	13	4.7	51	28	1.0	0.1	1.9
t1.5 A1	Silt loam	7.6	7.2	212	124	214	13	196	75	98	73	45	1.9	0.1	2.4
t1.6 A2	Silt loam	7.5	7.1	232	136	234	15	202	116	181	76	47	1.9	0.1	2.2

[a] Organic carbon

[b] Organic matter

Table 2 Mineralogical composition of the polluted soils (A1 and A2) and control (unpolluted)

Phase	Control	A1 (%)	A2
Illite	24	17	10
Kaolinite	8.4	3.0	5.7
Quartz	8.8	5.6	5.3
Albite	5.8	5.4	5.9
Rutile	1	0.7	0.7
Calcite	12	15	17
Amorphous	40	53	54

Table 4 DTPA-extractable concentrations of major and trace elements in the polluted soils (A1 and A2) and control (unpolluted)

	Control mg kg^{-1}	A1	A2
Cr	0.01	0.3	0.3
Mn	31	15	17
Fe	8.3	92	123
Ni	0.1	3.1	3.2
Cu	1.5	40	14
Zn	1.5	201	208
Cd	0.1	0.2	0.2
Pb	0.9	11	5

30 mg kg^{-1}; Cubadda et al. 2010). Unlike the control, both A1 and A2 were characterized by levels of Cr, Cu, Zn and Pb higher than the regulatory thresholds.

Assessment of chromium contamination

Chromium was the most abundant PTE in the investigated soils, with concentrations 25 (A1) and 34 (A2) times higher than the regulatory limits. However, Cr(VI) was not detected in these soils. A 0% spike recovery was obtained using USEPA methods 3060A and 7196A for Cr(VI) determination, both when adding a Cr(VI) spike of 40 mg kg^{-1} (as recommended in the method 3060A) and when using a Cr(VI) spike tenfold higher. Alkaline digestion method followed by the diphenylcarbazide colorimetric assay is the most common procedure adopted for Cr(VI) determination in soil (James et al. 1995). Nevertheless, the presence of high levels of OM in samples, as in A1 and A2, might negatively interfere with Cr(VI) quantification. The strong alkaline conditions of the method (pH 11.5) promote the extraction of soil humic substances, which rapidly reduce Cr(VI) under the strong acid conditions (pH 2) required for the colorimetric assay (Pettine and Capri 2005). Both for A1 and A2 samples, humic acids abundantly flocculated in the soil alkaline extracts during the acidification at pH 7.5; thus, extracts were filtered at 0.45 μm. Despite filtration, an evident flocculate formed again in the diphenylcarbazide-added extracts during the acidification at pH 2. Additional filtration of the diphenylcarbazide-added extracts at 0.22 μm was not resolutory, thus confirming the inadequacy of the method for matrices characterized by high content of humic substances.

The potential capacity of soil to oxidize Cr(III) to Cr(VI) was evaluated following the method described by Bartlett and James (1996). As stated by the Italian legislation (Italian Directive n. 99/ 1992), soil has to be considered at risk when, following the oxidation test, more than 1 μmol Cr(VI) is formed spiking 2 g of soil with 25 μmol Cr(III). Formation

Table 3 Elemental composition of the polluted soils (A1 and A2) and control (unpolluted)

		Major elements[a]											
		Na_2O	MgO	Al_2O_3	SiO_2	P_2O_5	SO_3	K_2O	CaO	TiO_2	MnO	Fe_2O_3	LOI[b]
		(%)											
	Control	0.6	1.2	19	41	0.2	0.3	2.7	8.5	0.8	0.2	6.6	19
	A1	0.4	1.0	10	26	1.0	1.5	1.8	13	0.5	0.1	6.2	38
	A2	0.4	0.9	11	26	1.6	2.1	1.7	16	0.5	0.1	6.8	33
		Trace elements[c]											
		Total Cr	Ni		Cu		Zn		As	Cd		Pb	
		mg kg^{-1}											
	Control	65 ± 11	54 ± 9		32 ± 4		69 ± 3		32 ± 2	0.5 ± 0.02		10 ± 3	
	A1	3807 ± 30	49 ± 9		342 ± 7		1173 ± 9		30 ± 3	0.8 ± 0.4		245 ± 4	
	A2	5160 ± 35	42 ± 9		134 ± 5		1270 ± 10		30 ± 2	0.8 ± 0.2		114 ± 3	
	Italian threshold[d]	150	120		120		150		20	2		100	

[a] Results of WD-XRF analysis

[b] Loss on ignition

[c] Results (mean ± standard deviation; $n = 3$) of ED-XRF analysis except Cd, which was determined by ICP-AES

[d] Maximum admissible limits for trace elements in soil according to the Italian regulation D.L. 152/06

JnlID 11356_ArtID 8857_Proof# 1 - 18/04/2020

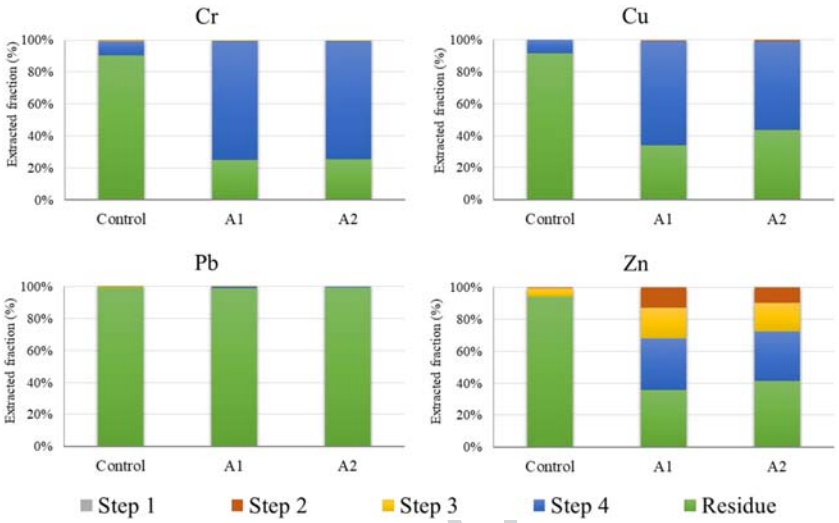

Fig. 1 Percentages of Cr, Cu, Pb and Zn extracted from the polluted soils (A1 and A2) and the control (unpolluted) after each step of BCR SEP. The four steps correspond to exchangeable (step 1), acid-soluble (step 2), reducible (step 3) and oxidisable (step 4) fractions

of Cr(VI) in both A1 and A2 was negligible (< 0.1 μmol), indicating the absence of any risk for Cr(III) oxidation. This behaviour might be attributed to the high content of easily oxidisable OM in A1 and A2, as well as to the potential presence of other reducing components, such as Fe(II)- and Mn(II)-oxides. Results of Cr(VI) determination and standard Cr net oxidation test jointly revealed that Cr was present in A1 and A2 soils in the trivalent form, and the extremely high content of soil OM hindered Cr oxidation.

Availability and fractionation of PTE

Chromium DTPA-extractable fraction was negligible in all the soils (Table 4), notwithstanding the high concentrations of total Cr in A1 and A2. This extraction method allows estimating the fraction of micronutrients and trace elements potentially accessible by plants and microorganisms. DTPA forms very stable complexes with metal cations present in soil as soluble, exchangeable and weakly complexed forms (Soriano-Disla et al. 2010). From obtained results, it can be deduced that Cr was not bioavailable in the two contaminated soils, being likely immobilized in the solid fraction, recalcitrant to the complexing action of DTPA. With regard to the other PTE, Zn and Cu DTPA-extractable fractions were relevant (up to 17% and 12% of their total concentrations, respectively). However, these values were not alarming, being Zn and Cu also essential plant micronutrients. Concentrations of Ni and Pb in the DTPA-extractable fraction of A1 and A2 soils were not negligible. The levels of potentially bioavailable Ni might pose a limited risk for plants, considering that Ni is also an essential micronutrient for higher plants, e.g. being a cofactor of urease (Hänsch and Mendel 2009; Gupta et al. 2017). Conversely, the concentrations of potentially bioavailable Pb might cause higher concern, being this element highly toxic for all living organisms.

Sequential chemical extractions revealed that Cr was almost completely distributed in the most recalcitrant soil fractions, namely the oxidisable (Cr bound to organic matter and/or sulphides) and the residual fractions (Fig. 1). The Cr fraction ascribable to these two phases changed moving from the unpolluted soil (control) to the polluted ones. In the control, 9% of the total Cr was associated to the oxidisable fraction and 90% to the residue, in accordance with the observations made by Köleli (2004) for a number of agricultural soils. Conversely, in the two contaminated soils, 74% of the total Cr was associated to the oxidisable fraction and 25% was retained in the residue. The large amount of OM in A1 and A2 played a crucial role in Cr immobilization by complexation mechanisms, as described by Wen et al. (2018). The XRPD analysis did not detect pure Cr-bearing minerals in soils (Table 2). Therefore, Cr in the residual fraction was likely attributable to Cr substituting Al in the octahedral sheets of illite and kaolinite (Bartlett and James 1996), as well as Cr-bearing cryptocrystalline structures and/or insoluble minerals at concentrations below the XRPD detection limit (thus quantified as amorphous components by XRPD).

Table 5 Distribution of PTEs in different particle-size fractions of the polluted soils A1 and A2

Soil fraction	Cr	Cu	Zn	Pb
	mg kg^{-1}			
Soil A1				
2000–500 μm	4108 ± 100[a]	256 ± 5	1165 ± 14	212 ± 21
500–125 μm	4145 ± 81	292 ± 18	1269 ± 8	245 ± 5
< 125 μm	3095 ± 21	294 ± 3	1198 ± 3	241 ± 2
Soil A2				
2000–500 μm	6489 ± 64	139 ± 1	1374 ± 16	146 ± 5
500–125 μm	4943 ± 99	133 ± 4	1252 ± 14	107 ± 6
< 125 μm	3600 ± 66	130 ± 3	1198 ± 14	98 ± 4

[a] Mean ± standard deviation ($n = 3$)

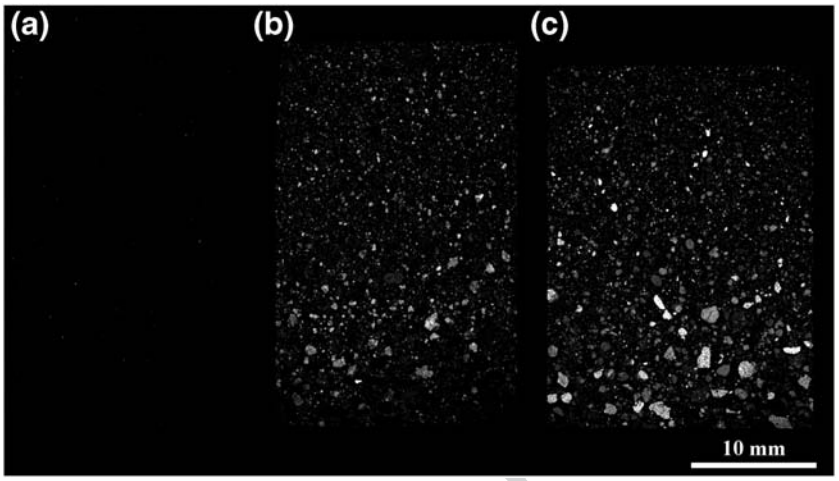

Fig. 2 Cr distribution maps acquired by μXRF for the unpolluted control soil (**a**), and the polluted soils A1 (**b**) and A2 (**c**). Brighter pixels correspond to higher Cr concentrations. All the maps use the same intensity scale and can be directly compared

Copper fractionation was similar to that of Cr, while Pb was almost totally (99%) immobilized in the soil residual fraction (Fig. 1), thus suggesting very limited environmental risk. Zinc mobility was negligible in the control, but moderate in A1 and A2, where Zn was found in the carbonate-bound fraction (11%, on average), in the reducible fraction (19%, on average), in the oxidisable fraction (31% on average) and in the residue (39% on average). Differences in PTE fractionation between the polluted and unpolluted soils might depend on both the different soil conditions (especially the content of OM and active carbonates) and origin of PTEs (natural vs anthropic).

Partitioning of Cr, Cu, Zn and Pb as a function of soil particle size is reported in Table 5. In A1 and A2, Cr concentration increased by 33% and 80%, respectively, moving from the finest fraction (< 125 μm) to the coarsest fraction (500 ÷ 2000 μm). This peculiar Cr distribution differs compared with what was reported in literature on PTE partitioning in soil (Qian et al. 1996; Wang et al. 2006; Parra et al. 2014). Indeed, PTE are usually more concentrated in the finest particles, because of their higher surface area and their higher content of reactive clay minerals, organic matter and Fe/Al/Mn oxides (Förstner and Salomons 1980; Qian et al. 1996). The peculiar distribution of Cr in coarse particles, for A1 and A2 soils, might be attributed to the origin of pollution. In fact, pollution of A1 and A2 was likely caused by the distribution on the soil of Cr-containing waste materials, possibly thoroughly mixed with organic amendments and buried in soil (see the "Origin of soil pollution" section).

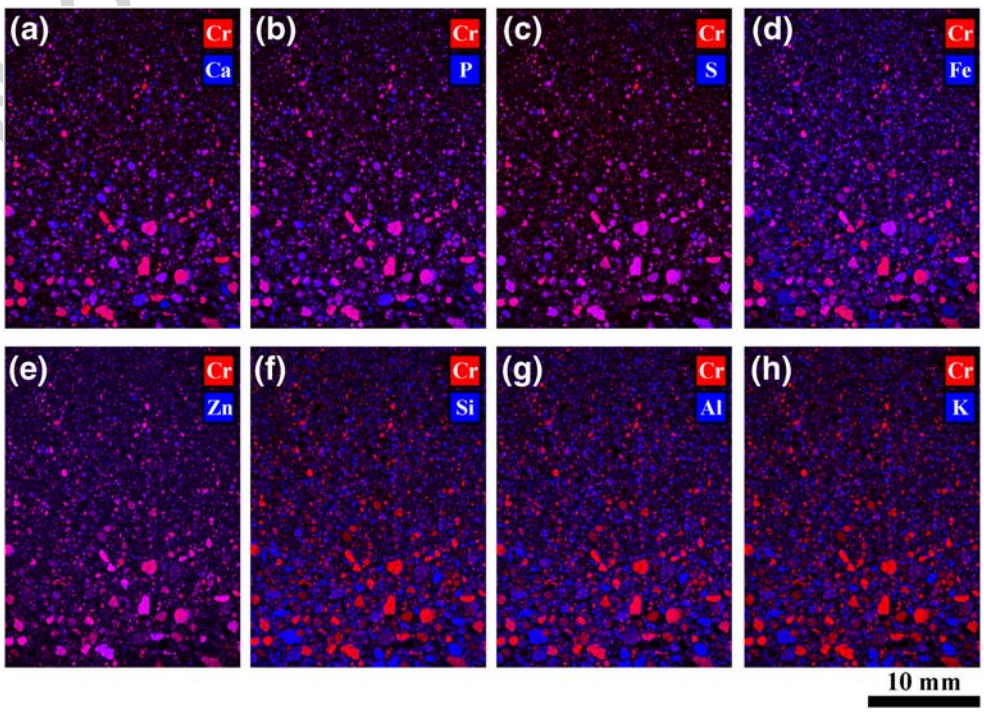

Fig. 3 Micro-XRF maps of the polluted soil A2 showing the distribution of Cr (in red) and its association with each of the following elements (in blue): Ca, P, S, Fe, Zn, Si, Al and K (**a**–**h**). Brighter pixels correspond to higher element concentrations

JnlID 11356_ArtID 8857_Proof# 1 - 18/04/2020

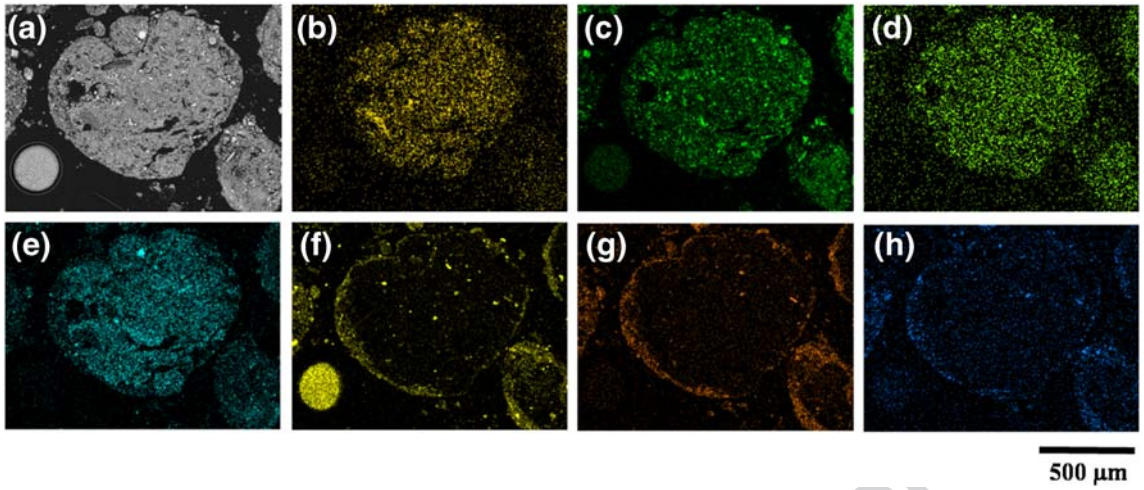

Fig. 4 FEGSEM micrograph of a Cr-containing aggregate of the polluted soil A2 (**a**), and related distribution EDX maps of Cr, Ca, P, Fe, Si, Al and K (**b**–**h**). Brighter pixels correspond to higher element concentrations

Copper was present in all the soil size fractions, without any specific distribution, as observed also by Yarlagadda et al. (1995) for Cu-polluted soils. Behaviour of Zn and Pb varied with soil sample. In particular, it was similar to that of Cr in A2, although less evident.

Micro-characterization of soils

Micro-XRF analysis of A1 and A2 thin sections (Figs. 2b, c) revealed that Cr was highly concentrated and homogenously distributed in soil aggregates with a size ranging from tens of micrometres to few millimetres, whereas no Cr-containing aggregate was detected in the control soil (only few microscopic bright spots, Fig. 2a). Because of the high similarity between µXRF results of A1 and A2 samples, only data of the most contaminated soil (A2) are hereafter shown and discussed. Overlapping of different element distribution maps revealed that Cr (displayed in red) was distributed in aggregates also containing Ca, P, S, Fe and Zn (Figs. 3a–e), as evidenced by the dominating purple colour of the section images (being blue the colour used to display the element other than Cr). It was also evident that Cr was not associated to Si, Al and K (Figs. 3f–h), as in these latter maps red and blue colours were clearly separated.

In order to better understand the chemical and structural properties of the Cr-containing aggregates, soil thin sections were also analysed by FEGSEM-EDX. Images acquired for a representative millimetre-sized aggregate of soil A2 are reported in Fig. 4. This aggregate was characterized by a compact structure and a well-defined contour (Fig. 4a). Elements, such as Cr, Ca, P and Fe, were rather homogenously distributed within the whole aggregate (Figs. 4b–e), although some small spots of Ca, Cr and Fe at higher concentrations were also visible. On the other hand, Si, Al and K were scarcely distributed in the inner portion of the aggregate, whereas they were more concentrated along the borders (Figs. 4f–h). Additional FEGSEM-EDX analyses were performed directly on millimetre-size soil aggregates isolated from the bulk soil and fixed on the stub, without incorporation in the epoxy resin and sectioning. Chemical mapping of the surface of these

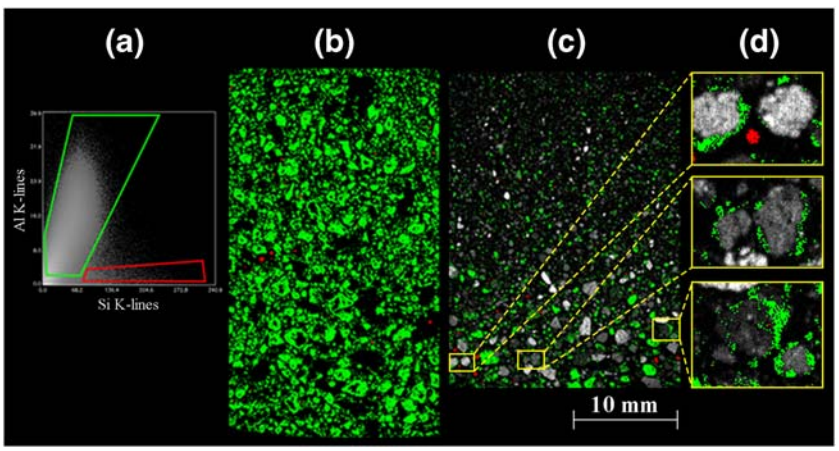

Fig. 5 **a** Total Al vs Si scatterplot obtained using fluorescent K-line signals of both B and C thin sections. Two different Al/Si ratios are visible: a high Al/Si ratio (green-bordered region) and a low Al/Si ratio (red-bordered region). Particles in the control sample (**b**) and A2 sample (**c**) having an Al/Si ratio belonging to the "green" or "red group". The grey areas correspond to the Cr distribution as in Fig. 2. **d** Magnification of the Cr particles surrounded by the "green" aluminosilicate fraction

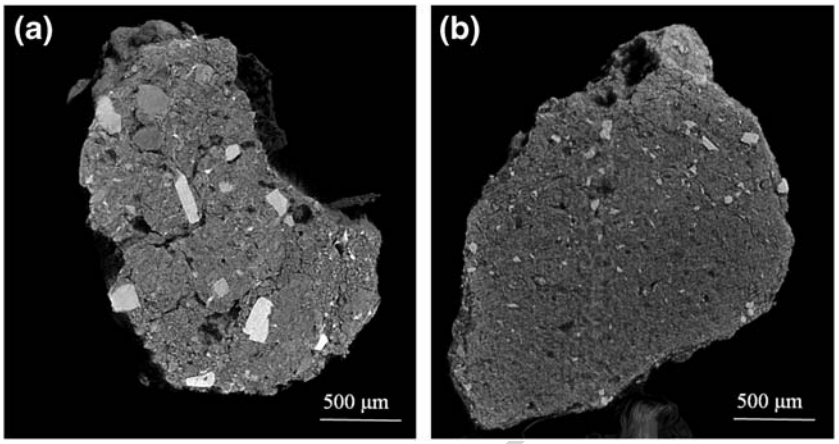

Fig. 6 Micro-CT images of a section of a soil aggregate isolated from the unpolluted control soil (**a**), and a soil aggregate isolated from the polluted A2 soil (**b**)

particles revealed the presence of Si, Al and K, but no signal of Cr (data not shown). All these results suggested that Cr was mostly concentrated inside the soil aggregates and that an aluminosilicate layer coated these aggregates. This type of aggregates was absent in the control, and therefore, it was reasonably of anthropogenic origin (see the "Origin of soil pollution" section).

To demonstrate this hypothesis, Al-Si scatterplots obtained from μXRF maps of control and A2 soils were compared, reporting the Cr map as background in grey scale (Figs. 5a–d). Control sample was characterized by the presence of aluminosilicate particles with relatively high Al/Si ratios (Fig. 5b, green), while the Cr-containing particles (grey) were negligible. A less relevant aluminosilicate fraction, characterized by very low Al/Si ratios, was also present in the control (Fig. 5b, red), and it was mostly attributable to quartz. Both these aluminosilicate fractions were present also in the polluted soil, although in completely different amounts (Fig. 5c). Compared with the control, in A2, the quantity of aluminosilicates with higher Al/Si ratios was much lower (Fig. 5c, green), whereas an additional fraction containing high concentrations of Cr and low concentrations of aluminosilicates prevailed (grey). Several Cr-containing particles were surrounded by the (green) aluminosilicate fraction (Figs. 5c–d), in agreement with the results obtained by FEGSEM-EDX analysis at higher spatial resolution. These evidences proved that the polluted soils contained an exogenous fraction (not present in the control), characterized by high levels of Cr, and an endogenous aluminosilicate fraction (also present in the control), which coated the Cr aggregates. In conclusion, these results suggest that waste materials containing large amounts of Cr were mixed with the agricultural soil, and over time, Cr was stabilized within large aggregates covered by endogenous aluminosilicate phases.

To further confirm the anthropogenic nature of the Cr-containing aggregates, millimetre-sized soil aggregates were isolated from both the control and A2 soil, and analysed by μCT. Indeed, a completely different morphology and inner structure were observed depending on the origin of the aggregate (Fig. 6a–b). The structure of Cr-bearing aggregates isolated from A2 (Fig. 6b) appeared more homogenous and compact, as well as characterized by the presence of few small mineral fragments, compared with the aggregates isolated from the control (Fig. 6a), which showed larger mineral fragments and a different texture. These noticeable differences further confirmed that the soil particles rich in Cr were allochthones.

Origin of soil pollution

Analyses by FEGSEM-EDX revealed the presence of Cr hotspots characterized by a fibrous morphology within the Cr-containing aggregates of the polluted soils (Figs. 4 and 7). These peculiar structures showed a high degree of similarity with SEM images acquired on cross-sections of goat leather by Kanagaraj et al. (2014) and Khandelwal et al. (2015).

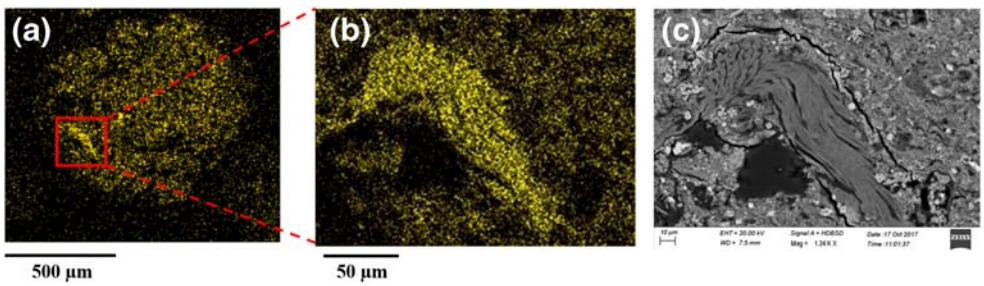

Fig. 7 FEGSEM-EDX Cr distribution map of the soil aggregate reported in Fig. 4 (**a**). Magnification on the Cr hotspot: Cr distribution map (**b**) and backscatter electrons micrograph (**c**)

JnlID 11356_ArtID 8857_Proof# 1 - 18/04/2020

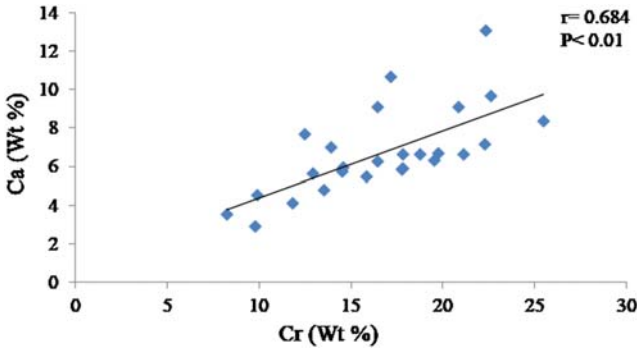

Fig. 8 Correlation diagram between Cr concentration and Ca concentration measured by FEGSEM-EDX in 26 points from six Cr-containing aggregates of the polluted soil A2

EDX chemical analysis on 26 points distributed on six different Cr-containing aggregates of the soil A2 revealed the occurrence of a significantly positive correlation between the concentration of Cr and Ca ($r = 0.684$, $P < 0.01$) (Fig. 8). Combining the microanalysis clues with outcomes of bulk analyses (i.e. the presence of abundant OM in the polluted soils and the preferred localization of Cr in the coarse soil fraction) allowed deducing that Cr pollution was likely caused by the discharge on soil of tanning industry by-products, possibly tannery sludge. The leather industry is the major cause of Cr inflow in the environment, accounting for 40% of the total industrial use (Barnhart 1997). More than 90% of leather goods are tanned with alkaline Cr(III) salts, principally $Cr_2(SO_4)_3$, and more than 60% of Cr used is discharged as solid and liquid wastes at the end of the tanning process (Kolomaznik et al. 2008). In most of cases, effluents produced after each step of the leather processing are mixed all together and finally subjected to chemical, physical and biological treatments, with the formation of a Cr-containing sludge which is difficult to reuse and, therefore, is disposed into dumps (Cassano et al. 2001). In other cases, Cr-bearing sludge is reused in agriculture as soil amendment or organic fertilizer, as it is or after composting (Ciavatta et al. 2012; Silva et al. 2014). The advantage of using such materials as fertilizers resides in their high content of organic C (38–50%, on average) and organic N (8–13%, on average), along with many other essential nutrients (P, K, Ca, S, Mg, Fe, Cu and Zn) (Ciavatta et al. 2012). As reported by Silva et al. (2014), composted tannery sludge is characterized not only by high concentrations of Cr, but also by a high content of Ca (100 g kg^{-1}, on average), possibly deriving from $Ca(OH)_2$ used for the leather liming. Indeed, Cr and Ca appeared always associated in the Cr-bearing aggregates of soils A1 and A2, with concentrations highly correlated between them (Fig. 8), thus confirming the hypothesis that soil pollution was caused by the landfill of Cr-containing tannery wastes, untreated or treated through physical, chemical or biological processes, including composting. According to the Italian legislation, no restriction for the agricultural use of Cr-containing tannery sludge exists, provided that the soil has no potential risk for Cr oxidation, and possesses suitable values of CEC and pH (Italian Directive n. 99/ 1992). Some limitations exist for composting, since only Cr-free tannery sludge can be composted (Italian Ministerial Decree n. 186/ 2006). However, pollution of the investigated area occurred before the introduction of such regulatory restrictions and illegal composting of Cr-containing sludge cannot be excluded.

Environmental implications

All the reported data suggest that, at present, there is limited environmental and human health concern associated with the high metal contamination of the investigated area. Chromium and most of PTE detected in the polluted soils appear immobilized by strong complexation with organic matter inside soil aggregates. The latter are further stabilized by an aluminosilicate layer, which has deposited on the waste materials over the years. The huge OM content does not allow oxidation of Cr(III) to more toxic Cr(VI). The appreciable amount of DTPA-extractable Pb fraction might pose some risks for plant species. Nevertheless, the agricultural activities, in particular the durum wheat cultivation, are still carried out on the site despite the high soil contamination. Previous studies on PTE accumulation in barley (*Hordeum vulgare*, L.) and wheat grown on the same site (Brunetti et al. 2012) showed that very low Cr, Pb, Ni, Cu, Zn and Cd concentrations are accumulated in straw and grain of cereals because of the very limited bioavailability of these elements, thus confirming a low risk for humans and animals. However, changes in OM structure and aggregate stability could cause the remobilisation of PTE, thus possibly determining the release of huge amounts of metal pollutants in the environment. In particular, OM turnover and biological mineralisation should be considered, as well as accidental or intentional fires which could cause OM burning and also lead to Cr(III) oxidation to Cr(VI).

Conclusions

The integrated analytical approach used in the present study allowed assessing the speciation of Cr in two PTE-polluted soils and hypothesising the origin of the soil pollution. Bulk analyses revealed extremely high concentrations of total Cr and OM in the polluted soils. DTPA and sequential extractions proved that Cr was immobilized in the most recalcitrant soil fractions, especially in OM. Risks of Cr oxidation to highly toxic hexavalent form were negligible, due to the high OM levels. Distribution of Cr in soil aggregates also containing Ca, P and Fe, and covered by an aluminosilicate layer, was observed by microanalyses. Elaborations of μXRF hyperspectral data revealed that a natural stabilization process

occurred in the investigated soils over the years, causing a sort of "capping" of Cr-containing particles with an aluminosilicate layer. The distribution of Cr in the coarser soil fractions ($\varnothing > 500$ μm), the very high content of OM, the presence of leather residues and the high concentrations of Ca in the Cr-containing aggregates jointly proved that soil pollution was most likely caused by the discharge of tannery waste-derived matrices in soil. The pool of information obtained combining bulk characterizations and microanalyses of PTEs-polluted soils is extremely useful to assess the dynamics of hazardous elements in soil and predict associated environmental risks. The present study allowed excluding environmental risks associated to the presence of Cr in the investigated soils, at least until high amounts of OM persist in the soil.

Acknowledgements The authors thank Mrs. Rosaria Mininni of the University of Bari for the technical support given in soil analyses. X-ray analyses were performed at the "Micro X-ray Lab" of the University of Bari. The work was supported by the Research Programme "FutureIn-Research" (Regione Puglia, Italy).

Author contributions Conceptualization: Concetta Eliana Gattullo and Roberto Terzano; Methodology: Concetta Eliana Gattullo, Ignazio Allegretta and Roberto Terzano; Formal analysis and investigation: Concetta Eliana Gattullo, Ignazio Allegretta, Carlo Porfido and Ida Rascio; Writing - original draft preparation: Concetta Eliana Gattullo; Reviewing: Matteo Spagnuolo and Roberto Terzano; Funding acquisition: Matteo Spagnuolo and Roberto Terzano; Supervision: Roberto Terzano.

Funding information This study was supported by the Research Programme "FutureIn-Research" (Regione Puglia, Italy).

Compliance with ethical standards

Conflict of interest The authors declare that they have no conflict of interest.

References

Alfeld M, Janssens K (2015) Strategies for processing mega-pixel X-ray fluorescence hyperspectral data: a case study on a version of Caravaggio's painting supper at Emmaus. J Anal Atom Spectrom 30:777–789. https://doi.org/10.1039/c4ja00387j

Allegretta I, Porfido C, Martin M, Barberis E, Terzano R, Spagnuolo M (2018) Characterization of As-polluted soils by laboratory X-ray-based techniques coupled with sequential extractions and electron microscopy: the case of Crocette gold mine in the Monte Rosa mining district (Italy). Environ Sci Pollut Res 25:25080–25090. https://doi.org/10.1007/s11356-018-2526-9

Barceló, J., and Poschenrieder, C. (1997) "Chromium in plants", in Chromium Environmental Issues, eds. S. Canali, F. Tittarelli, P. Sequi (Milano, Italy: FrancoAngeli s.r.l.), 101-129

Barnhart J (1997) Occurrences, uses, and properties of chromium. Regul Toxicol Pharmacol 26:3–7. https://doi.org/10.1006/rtph.1997.1132

Bartlett RJ, and James BR (1996) "Chromium, methods of soil analysis", in Methods of Soil Analysis, Part 3-Chemical Methods, ed. D. L. Sparks (Madison, WI: ASA/SSSA Press), 683-701

Bartlett RJ (1997). "Chromium redox mechanisms in soils: should we worry about Cr(VI)?", in Chromium Environmental Issues, eds. S. Canali, F. Tittarelli, P. Sequi (Milano, Italy: FrancoAngeli s.r.l.), 1–20

Becquer T, Quantin C, Sicot M, Boudot JP (2003) Chromium availability in ultramafic soils from New Caledonia. Sci Total Environ 301:251–261. https://doi.org/10.1016/S0048-9697(02)00298-X

Brunetti G, Farrag K, Soler-Rovira P, Ferrara M, Nigro F, Senesi N (2012) Heavy metals accumulation and distribution in durum wheat and barley grown in contaminated soils under Mediterranean field conditions. J Plant Interact 7:160–174. https://doi.org/10.1080/17429145.2011.603438

Cassano A, Molinari R, Romano M, Drioli E (2001) Treatment of aqueous effluents of the leather industry by membrane processes - a review. J Membr Sci 181:111–126. https://doi.org/10.1016/S0376-7388(00)00399-9

Ciavatta C, Manoli C, Cavani L, Franceschi C, Sequi P (2012) Chromium-containing organic fertilizers from tanned hides and skins: a review on chemical, environmental, agronomical and legislative aspects. J Environ Prot 3:1532–1541. https://doi.org/10.4236/jep.2012.311169

Cook KR (2000) In situ treatment of soil and groundwater contaminated with chromium – technical resource guide. EPA/625/R-00/005. U.S. Environmental Protection Agency Press, Ohio

Cubadda F, Ciardullo S, D'Amato M, Raggi A, Aureli F, Carcea M (2010) Arsenic contamination of the environment-food chain: a survey on wheat as a test plant to investigate phytoavailable arsenic in Italian agricultural soils and as a source of inorganic arsenic in the diet. J Agric Food Chem 58:10176–10183. https://doi.org/10.1021/jf102084p

Dhal B, Thatoi HN, Das NN, Pandey BD (2013) Chemical and microbial remediation of hexavalent chromium from contaminated soil and mining/metallurgical solid waste: a review. J Hazard Mater 250–251:272–291. https://doi.org/10.1016/j.jhazmat.2013.01.048

Ertani A, Mietto A, Borin M, Nardi S (2017) Chromium in agricultural soils and crops: a review. Water Air Soil Pollut 228:190. https://doi.org/10.1007/s11270-017-3356-y

Förstner U, Salomons W (1980) Trace metal analysis of polluted sediments. Environ Sci Technol Lett 1:494–505. https://doi.org/10.1080/09593338009384006

Gattullo CE, D'Alessandro C, Allegretta I, Porfido C, Spagnuolo M, Terzano R (2018a) Alkaline hydrothermal stabilization of Cr(VI) in soil using glass and aluminum from recycled municipal solid wastes. J Hazard Mater 344:381–389. https://doi.org/10.1016/j.jhazmat.2017.10.035

Gattullo CE, Pii Y, Allegretta I, Medici L, Cesco S, Mimmo T et al (2018b) Iron mobilization and mineralogical alterations induced by iron-deficient cucumber plants (*Cucumis sativus* L.) in a calcareous soil. Pedosphere 28:59–69. https://doi.org/10.1016/S1002-0160(15)60104-7

Gualtieri AF (2000) Accuracy of XRPD QPA using the combined Rietveld-RIR method. J Appl Crystallogr 33:267–278. https://doi.org/10.1107/S002188989901643X

Gupta V, Jatav PK, Verma R, Kothari SL, Kachhwaha S (2017) Nickel accumulation and its effect on growth, physiological and biochemical parameters in millets and oats. Environ Sci Pollut Res 24:23915–23925. https://doi.org/10.1007/s11356-017-0057-4

Hänsch R, Mendel RR (2009) Physiological functions of mineral micronutrients (Cu, Zn, Mn, Fe, Ni, Mo, B, Cl). Curr Opin Plant Biol 12:259–266. https://doi.org/10.1016/j.pbi.2009.05.006

Indorante SJ, Hammer RD, Koenig PG, Follmer LR (1990) Particle-size analysis by a modified pipette procedure. Soil Sci Soc Am J 54:560–563. https://doi.org/10.2136/sssaj1990.03615995005400020047x

Italian Directive n. 152/ (2006). Decreto legislativo 3 aprile 2006, n. 152. Norme in Materia Ambientale (Gazzetta Ufficiale Della Repubblica Italiana n. 88. Supplemento Ordinario n. 96, 14 aprile 2006)

Italian Directive n. 99/, (1992). Decreto legislativo 27 gennaio 1992, n. 99. Attuazione della direttiva 86/278/CEE concernente la protezione dell'ambiente, in particolare del suolo, nell'utilizzazione dei fanghi di depurazione in agricoltura (Gazzetta Ufficiale Della Repubblica Italiana n.28. Supplemento Ordinario n. 38, 15 Febbraio 1992)

Italian Ministerial Decree n. 186/, (2006). Decreto del Ministero dell'Ambiente e della Tutela del Territorio 5 aprile 2006, n. 186. Regolamento recante modifiche al decreto ministeriale 5 febbraio 1998 (Gazzetta Ufficiale della Repubblica Italiana n. 115, 19 maggio 2006)

IUSS Working Group WRB. 2006. World reference base for soil resources. World Soil Resources Reports No. 103. FAO, Rome

James BR, Petura JC, Vitale RJ, Mussoline GR (1995) Hexavalent chromium extraction from soils - a comparison of 5 methods. Environ Sci Technol 29:2377–2381. https://doi.org/10.1021/es00009a033

Kabata-Pendias, A., and Mukherjee, A. B. (2007). "Chromium", in Trace Elements from Soil to Human, eds. A. Kabata-Pendias, A.B. Mukherjee (Berlin Heidelberg, Germany: Springer Verlag), 173–183

Kanagaraj J, Tamil Selvi A, Senthilvelan T, Chandra Babu NK, Chandrasekar B (2014) Evaluation of new bacteriocin as a potential short-term preservative for goat skin. Am J Microbiol Res 2:86–93. https://doi.org/10.12691/ajmr-2-3-2

Khandelwal HB, More SV, Kalal KM, Laxman RS (2015) Eco-friendly enzymatic dehairing of skins and hides by *C. brefeldianus* protease. Clean Techn Environ Policy 17:393–405. https://doi.org/10.1007/s10098-014-0791-y

Köleli N (2004) Speciation of chromium in 12 agricultural soils from Turkey. Chemosphere 57:1473–1478. https://doi.org/10.1016/j.chemosphere.2004.08.068

Kolomaznik K, Adamek M, Andel I, Uhlirova M (2008) Leather waste—potential threat to human health, and a new technology of its treatment. J Hazard Mater 160:514–520. https://doi.org/10.1016/j.jhazmat.2008.03.070

Lindsay WL, Norwell WA (1978) Development of DTPA of soil test for Zn, Fe, Mn and Cu. J Am Soil Sci 42:421–428. https://doi.org/10.2136/sssaj1978.03615995004200030009x

Lombi E, Susini J (2009) Synchrotron-based techniques for plant and soil science: opportunities, challenges and future perspectives. Plant Soil 320:1–35. https://doi.org/10.1007/s11104-008-9876-x

Majumdar S, Peralta-Videa JR, Castillo-Michel H, Hong J, Rico CM, Gardea-Torresdey JL (2012) Applications of synchrotron μ-XRF to study the distribution of biologically important elements in different environmental matrices: a review. Anal Chim Acta 755:1–16. https://doi.org/10.1016/j.aca.2012.09.050

Mehta N, Cocerva T, Cipullo S, Padoan E, Dino GA, Ajmone-Marsan F, Cox SF, Coulon F, de Luca DA (2019) Linking oral bioaccessibility and solid phase distribution of potentially toxic elements in extractive waste and soil from an abandoned mine site: case study in Campello Monti, NW Italy. Sci Total Environ 651:2799–2810. https://doi.org/10.1016/j.scitotenv.2018.10.115

Morrison JM, Goldhaber MB, Lee L, Holloway JM, Wanty RB, Wolf RE, Ranville JF (2015) A regional-scale study of chromium and nickel in soils of northern California, USA. Appl Geochem 24:1500–1511. https://doi.org/10.1016/j.apgeochem.2009.04.027

Oze C, Fendorf S, Bird DK, Coleman RG (2004) Chromium geochemistry of serpentine soils. Int Geol Rev 46:97–126. https://doi.org/10.2747/0020-6814.46.2.97

Parra S, Bravo MA, Quiroz W, Moreno T, Karanasiou A, Font O, Vidal V, Cereceda F (2014) Distribution of trace elements in particle size fractions for contaminated soils by a copper smelting from different zones of the Puchuncaví Valley (Chile). Chemosphere 111:513–521. https://doi.org/10.1016/j.chemosphere.2014.03.127

Pettine M, Capri S (2005) Digestion treatments and risks of Cr(III)-Cr(VI) interconversions during Cr(VI) determination in soils and sediments - a review. Anal Chim Acta 540:231–238. https://doi.org/10.1016/j.aca.2005.03.040

Qian J, Shan X, Wang Z, Tu Q (1996) Distribution and plant availability of heavy metals in different particle-size fractions of soil. Sci Total Environ 187:131–141. https://doi.org/10.1016/0048-9697(96)05134-0

Sahuquillo A, López-Sánchez JF, Rubio R, Rauret G, Thomas RP, Davidson CM, Ure AM (1999) Use of certified reference material for extractable trace metals to assess sources of uncertainty in the BCR three-stage sequential extraction procedure. Anal Chim Acta 382:317–327. https://doi.org/10.1016/S0003-2670(98)00754-5

Shahid M, Shamshad S, Rafiq M, Khalid S, Bibi I, Niazi NK, Dumat C, Rashid MI (2017) Chromium speciation, bioavailability, uptake, toxicity and detoxification in soil-plant system: a review. Chemosphere 178:513–533. https://doi.org/10.1016/j.chemosphere.2017.03.074

Shanker AK, Cervantes C, Loza-Tavera H, Avudainayagam S (2005) Chromium toxicity in plants. Environ Int 31:739–753. https://doi.org/10.1016/j.envint.2005.02.003

Silva MDM, Barajas-Aceves M, Araújo ASF, Araújo FF, Melo WJ (2014) Soil microbial biomass after three-year consecutive composted tannery sludge amendment. Pedosphere 24:469–475. https://doi.org/10.1016/S1002-0160(14)60033-3

Solé VA, Papillon E, Cotte M, Walter P, Susini J (2007) A multiplatform code for the analysis of energy-dispersive X-ray fluorescence spectra. Spectochim Acta B 62:63–68. https://doi.org/10.1016/j.sab.2006.12.002

Soriano-Disla JM, Speir TW, Gómez I, Clucas LM, McLaren RG, Navarro-Pedreño J (2010) Evaluation of different extraction methods for the assessment of heavy metal bioavailability in various soils. Water Air Soil Pollut 213:471–483. https://doi.org/10.1007/s11270-010-0400-6

Sparks DL (1996) Methods of soil analysis, part 3, chemical methods. In: SSSA Book Series No 5. ASA/SSSASA Press, Madison

Terzano R, Spagnuolo M, Vekemans B, De Nolf W, Janssens K, Falkenberg G et al (2007) Assessing the origin and fate of Cr, Ni, Cu, Zn, Pb, and V in an industrial polluted soil by combined microspectroscopic techniques and bulk extraction methods. Environ Sci Technol 41:6762–6769. https://doi.org/10.1021/es070260h

Terzano R, Denecke MA, Falkenberg G, Miller B, Paterson D, Janssens K (2019) Recent advances in analysis of trace elements in environmental samples by X-ray based techniques (IUPAC technical report). Pure Appl Chem 91:1029–1063. https://doi.org/10.1515/pac-2018-0605

Thouin H, Le Forestier L, Gautret P, Hube D, Laperche V, Dupraz S et al (2016) Characterization and mobility of arsenic and heavy metals in soils polluted by the destruction of arsenic-containing shells from the Great War. Sci Total Environ 550:658–669. https://doi.org/10.1016/j.scitotenv.2016.01.111

USEPA, Method 3060A (1996). Alkaline digestion for hexavalent chromium. Washington: United States Environmental Protection Agency

USEPA, Method 7196A (1992) Chromium, hexavalent (colorimetric). United States Environmental Protection Agency, Washington

Vanhoof C, Corthouts V, Tirez K (2004) Energy-dispersive X-ray fluorescence systems as analytical tool for assessment of contaminated soils. J Environ Monit 6:344–350. https://doi.org/10.1039/b312781h

Wang X-S, Qin Y, Chen Y-K (2006) Heavy meals in urban roadside soils, part 1: effect of particle size fractions on heavy metals partitioning. Environ Geol 50:1061–1066. https://doi.org/10.1007/s00254-006-0278-1

Wen J, Li Z, Huang B, Luo N, Huang M, Yang R, Zhang Q, Zhai X, Zeng G (2018) The complexation of rhizosphere and nonrhizosphere soil organic matter with chromium: using elemental analysis combined

with FTIR spectroscopy. Ecotox Environ Safe 154:52–58. https://doi.org/10.1016/j.ecoenv.2018.02.014

Wong JWC, Li K, Fang M, Su DC (2001) Toxicity evaluation of sewage sludges in Hong Kong. Environ Int 27:373–380. https://doi.org/10.1016/S0160-4120(01)00088-5

Yarlagadda PS, Matsumoto MR, VanBenschoten JE, Kathuria A (1995) Characteristics of heavy metals in contaminated soils. J Environ Eng 121:276–286. https://doi.org/10.1061/(ASCE)0733-9372(1995)121:4(276)

AUTHOR QUERIES

AUTHOR PLEASE ANSWER ALL QUERIES.

Q1. Please check if the presentation and sequence (i.e., extended given name, middle name/initial, family name) of author names are accurate. Also, kindly confirm correctness of details in the metadata.
Q2. Please check if the affiliation is presented correctly.
Q3. The citation “Morrison et al., 2009” has been changed to “Morrison et al., 2015” to match the author name/date in the reference list. Please check if the change is fine in this occurrence and modify the subsequent occurrences, if necessary.
Q4. The citation “Cook et al., 2000” has been changed to “Cook, 2000” to match the author name/date in the reference list. Please check if the change is fine in this occurrence and modify the subsequent occurrences, if necessary.
Q5. The citation “Barceló and Poschenrieder, 2007” has been changed to “Barceló and Poschenrieder, 1997” to match the author name/date in the reference list. Please check if the change is fine in this occurrence and modify the subsequent occurrences, if necessary.
Q6. The citation “USEPA Method 3060A” has been changed to “USEPA, Method 3060A, 1996” to match the author name/date in the reference list. Please check if the change is fine in this occurrence and modify the subsequent occurrences, if necessary.
Q7. The citation “USEPA Method 7196A” has been changed to “USEPA, Method 7196A, 1992” to match the author name/date in the reference list. Please check if the change is fine in this occurrence and modify the subsequent occurrences, if necessary.